electron-donating or electron-accepting substituents when present alone.

## Summary

Data presented in this paper constitute the first nonkinetic experimental observations of nonadditive and synergistic substituent effects on the homolytic strengths of labile $sp^3$ C-H bonds and provide evidence for the significance of solvent-induced stabilization of appropriately substituted carbon-centered radicals. The nonadditivities present in the $sp^3$ C-H bond strengths for donor-acceptor-substituted species **4** and **6** (2 and 4 kcal/mol, respectively), although small in magnitude, are best explained by postulating that DMSO interacts with the donor-acceptor-substituted radicals **4** - **H**• and **6** - **H**• in a fashion that results in an enhanced stabilization for these species.

## Experimental Section

The syntheses of **2-8** and **10** were carried out in our laboratories and have been described previously.[15,16,31] 9-Methylanthracene (**1**, crystallized from EtOH) and phenylacetonitrile (**9**, distilled) were purchased from Aldrich.

All of the $pK_a$ values in Table I have been published previously; appropriate references for these values are listed in Table I.

Dimethyl sulfoxide was purified and potassium dimsylate was synthesized exactly as described by Matthews and Bordwell.[39] $Et_4N^+BF_4^-$ was recrystallized from acetone and was allowed to dry at 110 °C under vacuum prior to dissolution in DMSO. $Et_4N^+ClO_4^-$ was recrystallized from ethanol/water and dried under vacuum overnight prior to dissolution in DMSO.

(39) Matthews, W. S.; Bares, J. E.; Bartmess, J.; Bordwell, F. G.; Cornforth, F. J.; Drucker, G. E.; Margolin, Z.; McCallum, G. J.; Vanier, N. R. *J. Am. Chem. Soc.* **1975**, *97*, 7006-7014.

Electrochemistry conditions: all experiments were carried out in DMSO solution under an argon atmosphere as described previously.[16,17] 0.1 M $Et_4N^+BF_4^-$ and 0.1 M $Et_4N^+ClO_4^-$ were employed as electrolytes. The strongly basic anions derived from 9-methylanthracene, 9-(methoxymethyl)anthracene, and 9-(phenoxymethyl)anthracene were less stable in the presence of $Et_4N^+BF_4^-$, necessitating usage of the perchlorate salt as electrolyte for the anodic oxidations of these species. A standard three-electrode cell consisting of platinum working and auxiliary electrodes and a Ag/AgI reference electrode was used in the cyclic voltammetry (CV) oxidations. The ferrocene/ferrocenium redox couple at +0.875 V provided an internal standard of comparison for the $E_{ox}$ values in Table I. In the electrochemical cell, the carbanions were generated by addition of a stock solution of potassium dimsylate solution (ca. 0.15 M in DMSO) to a 7-8 mL solution of the acid to be deprotonated. The anions were present in 1-2 mM concentrations. The $E_{ox}$ values are the anodic peak potentials (CV sweep rate = 0.1 V/s) as reported by a BAS 100A electrochemical analyzer. The CV anodic peak potentials used in the calculations of the $\Delta E_{ox(C^-)}$ and $\Delta BDE_{(C-H\ homo)}$ values for **1-10** were reproducible to within 10 mV.

**Acknowledgment**. We are grateful to the United States Department of Energy (Office of Basic Energy Science), the donors of the Petroleum Research Fund, administered by the American Chemical Society, and the Illinois Department of Energy and Natural Resources for support of this work.

**Registry No. 1**, 779-02-2; **1** (carbanion), 122128-04-5; **2**, 1467-01-2; **2** (carbanion), 135598-24-2; **3**, 2584-79-4; **3** (carbanion), 135598-25-3; **4**, 133322-46-0; **4** (carbanion), 135598-26-4; **5**, 16430-34-5; **5** (carbanion), 135598-27-5; **6**, 135598-22-0; **6** (carbanion), 135598-28-6; **7**, 2961-76-4; **7** (carbanion), 135598-29-7; **8**, 135598-23-1; **8** (carbanion), 135598-30-0; **9**, 140-29-4; **9** (carbanion), 18802-89-6; **10**, 13031-13-5; **10** (carbanion), 95339-45-0; **4-H**•, 135619-07-7; **6-H**•, 135598-31-1.

# Low-Temperature X-ray and Neutron Diffraction Studies on 18-Crown-6·2 Cyanamide Including Electron Density Determination†

**T. Koritsânszky, J. Buschmann, L. Denner, P. Luger, A. Knöchel,* M. Haarich, and M. Patz**

*Contribution from the Central Research Institute for Chemistry of the Hungarian Academy of Sciences, H-1025 Budapest, Hungary, Institute for Crystallography, Free University of Berlin, D-1000 Berlin 33, Germany, and Institute of Inorganic and Applied Chemistry, University of Hamburg, D-2000 Hamburg 13, Germany.* *Received November 19, 1990*

**Abstract:** Low-temperature (100 K) X-ray and neutron diffraction data have been combined to obtain accurate molecular dimensions and to study the charge density distribution in the neutral complex of 18-crown-6 and cyanamide. Conformational changes in the polyether ring as well as in the cyanamide molecule, due to complex formation, have been analyzed. The leading forces of complexation were found to be cooperative hydrogen bonds of different types and dipole–dipole interactions. Atomic valence deformations, due to chemical bonds and intermolecular interactions, were analyzed in terms of static and dynamic difference densities calculated by the fitted multipole model and X–X Fourier synthesis. In the deformation charge density maps well-defined bond peaks can be observed. Excess density in the regions associated with lone-pair electrons is found for the ether oxygen atoms. For those which participate in hydrogen bonding the maximum charge buildup is located in the direction of the proton. No further density accumulation is observed between the donor and the acceptor which supports the assumption about the electrostatic nature of the hydrogen bond. For the cyanamide molecule the experiment and the theory are in good agreement.

## Introduction

Macrocyclic polyethers like 18-crown-6 are known to complex not only cations but also neutral, polarized compounds. Several complexes of this kind with 1:2 stoichiometric ratio of host and guest have been prepared recently. The guest partners usually have high dipole moments and are coordinated above and below the crown in such a way that the dipoles are compensated. To describe this formation, a system of cooperative intermolecular contacts, as dipole–dipole interactions and hydrogen bonds, was postulated.[1]

† Dedicated to Professor Dr. Erwin Weiß on the occassion of his 65th birthday.

(1) Elbasyouny, A.; Brügge, H. J.; von Deuten, K.; Dickel, M.; Knöchel, A.; Koch, K. U.; Kopf, J.; Melzer, D.; Rudolph, G. *J. Am. Chem. Soc.* **1983**, *105*, 6568-6577.

0002-7863/91/1513-8388$02.50/0 © 1991 American Chemical Society

**Table I.** Crystal Data and Experimental Conditions for 18-Crown-6·2Cyanamide

| | X-ray | neutron |
|---|---|---|
| formula | $C_{12}H_{24}O_6(H_2NCN)_2$ | |
| formula wt | 348.4 | |
| space group | $P2_1/c$ | |
| $Z$ | 2 | |
| $d_{calc}$ (g/cm$^3$) | 1.266 | 1.267 |
| cell dimensions | | |
| $a$ (Å) | 8.084 (5) | 8.073 (2) |
| $b$ (Å) | 14.362 (10) | 14.359 (4) |
| $c$ (Å) | 7.939 (5) | 7.950 (2) |
| $\beta$ (deg) | 97.63 (3) | 97.62 (2) |
| $V$ (Å$^3$) | 913.58 (2) | 913.43 (1) |
| $F(000)$ | 376. | |
| $T$ (K) | 100 (1) | 100.00 (3) |
| abs coeff (cm$^{-1}$) | 1.09 | 2.23 |
| cryst dim. (mm) | 0.4 × 0.4 × 0.6 | 1.7 × 2.0 × 1.3 |
| vol (mm$^3$) | 0.056 | 4.42 |
| wave length (Å) | 0.71068 | 0.8453 |
| $\theta_{min} - \theta_{max}$ (deg) | 2–50 | 3–45 |
| $(h,k,l)$ min | −17,−21,−12 | −13,−24,−11 |
| $(h,k,l)$max | 10,0,12 | 12,2,13 |
| sin $\theta/\lambda_{max}$ (Å−1) | 1.0803 | 0.8362 |
| scan type | $\Omega$–$2\theta$ | $\Omega$–$2\theta$ |
| scan width (deg) | 1.5 + 0.26tan $\theta$ | 1.55 |
| scan rate (deg/min) | 0.5–2.0 | 1.3 |
| orientation reflcn | 21 | 6 |
| $\theta$ range (deg) | $21 < 2\theta < 48$ | $12 < 2\theta < 41$ |
| number of reflcns collected | 5383 | 4717 |
| number of unique reflcns | 3541 | 3211 |

These complexes may help to promote the understanding of the molecular recognition of nonionic polar moieties, which play an important role in molecular biology.[2] Therefore, in order to further investigate the bonding properties the electron density distribution of the title host–guest complex was studied.

## Experimental Section

**Neutron Measurement.** The neutron data were collected at the high flux reactor of the Institute Laue-Langevin in Grenoble on the D9 four-circle diffractometer with transmission monochromated radiation from a Cu crystal (reflection 220) and euipped with a two-stage Displex cooling unit, set to 100.0 K. Several reflections were used to check for anisotropic extinction and multiple reflection by $\psi$ scan measurement. After absorption correction negligible azimuthal variation was observed. In the range $38° \leq \theta \leq 45°$ only the 450 strongest peaks were collected. The two test reflections, measured once every 2 h, showed no systematic variation. Reflection profiles were evaluated by the COLLEGE v data reduction program package of M. Lehmann and S. Wilson.[3,4] The peak position, the background, the net intensity, and the standard deviation were calculated with the minimal $\sigma(I)/I$ method. An analytical absorption correction was applied with a Gaussian grid integration.[5] The data averaging was done with the SHELX76[6] program. The agreement index for averaging the equivalent reflections was 0.0208.

**X-ray Measurement.** X-ray data were collected at 100 (1) K with Zr filtered Mo K$\alpha$ radiation on a Siemens four-circle diffractometer equipped with a nitrogen gas stream cooling device designed by H. Dietrich.[7] The crystal was placed in a thin-walled glass capillary. Six check reflections were measured every 60 min. When the intensity of any check reflection dropped by at least 3%, the 21 reflections used in the refinement of the cell parameters were automatically recentered, and the orientation matrix was recalculated. This occurred about twice a day. No absorption correction was made because the linear absorption coefficient is small and the crystal shape was bulky. The merging of the equivalent reflections was done with the XTAL[8] program system, giving an agreement index of 0.017. Crystal data and experimental conditions for both measurements are given in Table I.

**Table II.** Summary of Refinements

| | neutron | spherical atom I | spherical atom II | multipole |
|---|---|---|---|---|
| min sin $\theta/\lambda$ | 0.0 | 0.0 | 0.65 | 0.0 |
| max sin $\theta/\lambda$ | 0.8362 | 1.0803 | 1.0803 | 1.0803 |
| no. of reflcns $\{\|F\| > 3\sigma(\|F\|)\}$ | 2700 | 3149 | 1639 | 3149 |
| no. of variables | 236 | 165 | 109 | 253 |
| $R$ | 0.0482 | 0.0402 | 0.0419 | 0.0229 |
| $R_w$ | 0.0442 | 0.0299 | 0.0278 | 0.0147 |

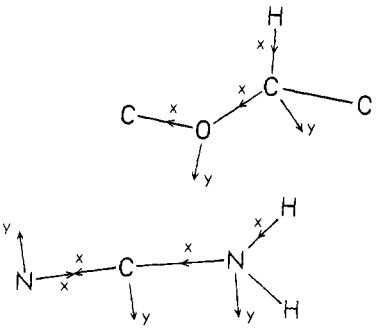

**Figure 1.** The local atomic coordinate systems used in multipole refinement.

## Structure Refinements

**Conventional Refinements.** Structural data obtained from a room-temperature measurement[1] gave a set of starting atomic parameters. Details of various refinements carried out on neutron and X-ray data are summarized in Table II. For both data sets the function $\sum_H w_H(|F_{obs}(H)| - k|F_{calc}(H)|)^2$ was minimized by the full-matrix least-squares method. Scattering factors, including those for anomalous scattering and the contracted function for the hydrogen, were taken from ref 9.

To fit the X-ray data both spherical and multipole atom models were tested. For the conventional X-ray refinement with all observed data the thermal motion of the hydrogen atoms was described isotropically. The spherical refinement gives a significantly shorter mean C–C (1.499 (1) Å) and C(1)–N(1) (1.139 (1) Å) and a slightly longer mean C–O (1.424 (1) Å) bond length than the fit to the neutron data. The latter longer bond is accompanied by a slight lowering of the mean C–O–C angle (112.1 (1)°). To reduce bias in the variables due to valence asphericity a refinement on high-order reflections (sin $\theta/\lambda > 0.65$ Å$^{-1}$) was carried out, keeping all hydrogen atom parameters fixed at the neutron values. The obtained geometrical parameters show better agreement with the neutron results except for the vibrational tensor elements which are 25% higher.

**Multipole Refinement.** The aspherical atomic density $\rho(r)$ is described in terms of spherical harmonics[10,11]

$$\rho(r) = P_c\rho_c(r) + P_v\kappa^3\rho_v(\kappa r) + \sum_{l=0}^{4} R_l(\kappa' r) \sum_{m=-l}^{l} P_{lm} y_{lm}(r/r)$$

where $\rho_c$ and $\rho_v$ are the spherical Hartree–Fock core and valence densities, $R_l$ and $y_{lm}$ stand for the Slater-type radial and the real normalized angular functions. Beside the conventional crystallographic parameters the $P_v$ and $P_{lm}$ populations as well as the $\kappa$ and $\kappa'$ expansion-contraction variables can be refined. The Fourier–Bessel transforms $\langle J_0 \rangle$ of $\rho_c$ and $\rho_v$ are given in ref 9; the parameters for the Slater orbitals were taken from ref 11. To reduce the number of parameters to be refined, the populations of chemically equivalent atoms were constrained to be equal. These constraints were applied to all carbon and hydrogen atoms

(2) Lehn, J.-M.; Simon, J.; Wagner, J. *Angew. Chem., Int. Ed. Engl.* **1973**, *12*, 578.
(3) Lehmann, M. S.; Larsen, F. K. *Acta Crystallogr.* **1974**, *A30*, 580.
(4) Lehmann, M. S. *J. Appl. Cryst.* **1975**, *8*, 619.
(5) Coppens, P.; Hamilton, W. C. *Acta Crystallogr.* **1970**, *A26*, 71.
(6) Sheldrick, G. M. *SHELX76: A Program for Crystal Structure Determination*; University of Cambridge, England, 1976.
(7) Dietrich, H.; Dierks, H. *Messtechnik (Braunschweig)* **1970**, *78*, 184.
(8) *XTAL2.2 User's Manual*; Hall, S. R., Stewart, J. M., Eds.; University of Western Australia, Nedlands, WA and University of Maryland, College Park, MD, 1987.
(9) International Tables for X-ray Crystallography IV; Ibers, J. A., Hamilton, W. C., Eds.; The Kynoch Press: Birmingham, England, 1974; pp 72–73, 102, 149.
(10) Stewart, R. F. *J. Chem. Phys.* **1969**, *51*, 4569.
(11) Hansen, N. K.; Coppens, P. *Acta Crystallogr.* **1978**, *A34*, 909.

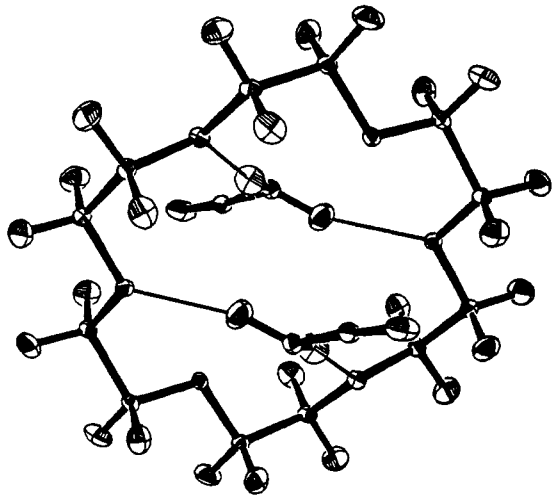

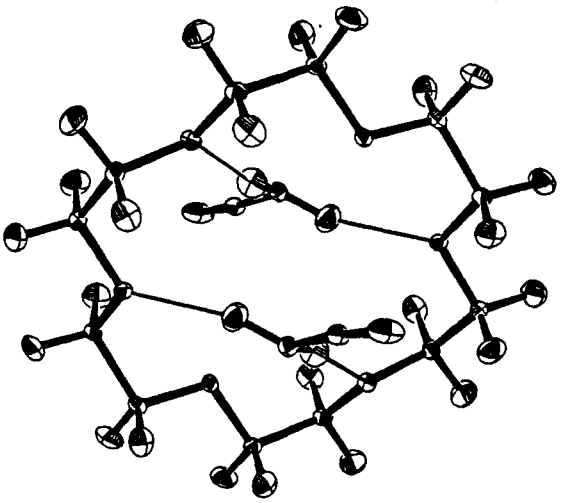

Figure 2. ORTEP drawing of the 18-crown-6·2cyanamid complex.

of the crown. The oxygen atoms were not constrained to allow for valence deformations due to a hydrogen bridge. To describe part of the bond densities the non-hydrogen atoms were treated up to the hexadecapolar level. To represent the deformation density at a hydrogen atom a dipole along the bond was applied. The positional and thermal parameters of the hydrogen atoms were fixed at the values obtained from the neutron data refinement. The definitions of the local coordinate systems are illustrated in Figure 1. In this local frame a $C_s$ site symmetry was assumed for each of the C and O atoms in the crown. In comparison to the spherical-atom model the multipole refinement gave an improved agreement (Table II). Final positional and thermal parameters are listed in Tables III and IV.

**Thermal-Motion Analysis.** TLS vibrational tensors[12] for the crown were obtained by a fit of a rigid-body motion model to the neutron thermal parameters (Table V). The main contribution is translational, but the poor agreement factor suggests that the internal modes should not be neglected. A better fit was achieved for the cyanamide molecule. But its librational tensor elements were not significant, indicating that the thermal motion of the bonded guest is far from being free. The same analysis, with the thermal parameters obtained after multipole fit to the X-ray data, gave similar results. It is important to note that the difference between X-ray and neutron thermal parameters could fairly well be described by the translational component. This indicates systematic errors in the reflection intensities, which are most likely due to thermal diffuse scattering (tds). The neglect of a tds correction results in an artifical reduction of the overall temperature factor. As it appears, by comparing the atomic mean squared displacements (msd) obtained by the two technics the inelastic scattering seems to be more intense for the neutron than for the X-ray case. Some confidence that this argument applies in the present case was gained from the thermal motion analysis that showed an important point: although the thermal parameters are indeed affected by some systematic error, its influence, however, is approximately the same for all atoms and accumulated in the translation tensor. In other words, the residual msd's $\Delta U_X$ and $\Delta U_N$ ($\Delta U = U_{obs} - U_{calc}$ (TLS)) from the two experiments show significant agreement which is especially important in view of obtaining "unbiased" charge density parameters.

The rigid-bond test proposed by F. L. Hirshfeld[13] was applied during the aspherical refinement to check for a correlation between the atomic msd's and the multipole parameters. When all but the screening parameters were refined, the thermal amplitudes satisified the rigid-bond postulate. When the $\kappa$ parameters were included in the refinement, a 5–6% expansion in the HF radial functions occurred with increased correlation coefficients between the multipole populations and msd's for the atoms in the crown.

Table III. Fractional Coordinates and Esd's[a]

| atom | x/a | y/b | z/c |
|---|---|---|---|
| O(1) | −0.3282 (1) | 0.0419 (1) | −0.1747 (1) |
| | −0.32731 (6) | 0.04170 (6) | −0.1737 (1) |
| C(2) | −0.3299 (1) | 0.12132 (9) | −0.2814 (1) |
| | −0.32986 (6) | 0.12122 (4) | −0.28030 (6) |
| C(3) | −0.2444 (1) | 0.20081 (8) | −0.1802 (1) |
| | −0.24407 (6) | 0.20036 (4) | −0.17887 (6) |
| O(4) | −0.0737 (1) | 0.17831 (9) | −0.1404 (1) |
| | −0.0737 (1) | 0.17801 (6) | −0.13959 (6) |
| C(5) | 0.0201 (1) | 0.25058 (8) | −0.0490 (1) |
| | 0.01968 (6) | 0.25017 (3) | −0.04848 (6) |
| C(6) | 0.2007 (1) | 0.22137 (8) | −0.0189 (1) |
| | 0.19992 (6) | 0.22140 (3) | −0.01835 (6) |
| O(7) | 0.2189 (1) | 0.14582 (9) | 0.0985 (1) |
| | 0.2184 (1) | 0.14567 (5) | 0.09877 (7) |
| C(8) | 0.3878 (1) | 0.11924 (8) | 0.1417 (1) |
| | 0.38728 (6) | 0.11912 (3) | 0.14114 (7) |
| C(9) | 0.3974 (1) | 0.03793 (9) | 0.2636 (1) |
| | 0.39720 (6) | 0.03825 (4) | 0.26281 (7) |
| N(1) | −0.1026 (1) | 0.05166 (6) | 0.1519 (1) |
| | −0.1016 (1) | 0.05132 (7) | 0.1538 (1) |
| C(1) | −0.1422 (1) | −0.00629 (9) | 0.2692 (1) |
| | −0.1423 (1) | −0.00667 (8) | 0.2708 (1) |
| N(2) | −0.1866 (1) | −0.05285 (9) | 0.3732 (1) |
| | −0.1881 (2) | −0.0534 (1) | 0.3743 (2) |
| H(21) | −0.2643 (4) | 0.1057 (2) | −0.3913 (3) |
| H(22) | −0.4606 (3) | 0.1404 (2) | −0.3286 (4) |
| H(31) | −0.3019 (3) | 0.2118 (2) | −0.0629 (3) |
| H(32) | −0.2594 (4) | 0.2657 (2) | −0.2552 (4) |
| H(51) | −0.0264 (3) | 0.2638 (2) | 0.0722 (3) |
| H(52) | 0.0088 (4) | 0.3154 (1) | −0.1239 (4) |
| H(61) | 0.2754 (3) | 0.2812 (2) | 0.0348 (4) |
| H(62) | 0.2427 (3) | 0.2001 (2) | −0.1389 (3) |
| H(81) | 0.4432 (3) | 0.1000 (2) | 0.0274 (4) |
| H(82) | 0.4596 (3) | 0.1785 (2) | 0.2036 (4) |
| H(91) | 0.3271 (4) | 0.0546 (2) | 0.3696 (3) |
| H(92) | 0.5290 (3) | 0.0248 (2) | 0.3138 (4) |
| H(1) | 0.0180 (3) | 0.0705 (2) | 0.1527 (4) |
| H(2) | −0.1654 (4) | 0.0438 (2) | 0.0344 (3) |

[a] Upper line, neutron; lower line, multipole refinement. Entries for the hydrogen atoms are based on the neutron observation.

In addition, the $U$ tensors obtained violated the rigid-bond condition in particular for the C–O bonds ($\Delta_{ab} \approx 2\text{–}3 \times 10^{-3}$ Å$^2$). In order to avoid this kind of bias, the conventional parameters were kept fixed in the final cycle of the multipole refinement.

**Molecular Structure.** An ORTEP[14] drawing of the complex is given in Figure 2. The final geometrical parameters of the polyether and the cyanamide molecule are listed in Tables VI and

(12) Trueblood, K. N. *Acta Crystallogr.* **1978**, *A34*, 950.
(13) Hirshfeld, F. L. *Acta Crystallogr.* **1976**, *A32*, 239.
(14) Johnson, C. K. ORTEP: A FORTRAN Thermal-Ellipsoid Plot Program for Crystal Structure Illustrations. Oak Ridge National Laboratory, ORN 2-3794, 1970.

**Table IV.** Temperature Factors (Å²) and Esd's[a,b]

| atom | U(1,1) | U(2,2) | U(3,3) | U(1,2) | U(1,3) | U(2,3) |
|---|---|---|---|---|---|---|
| O(1) | 0.0207 (6) | 0.0178 (6) | 0.0150 (5) | −0.0007 (4) | 0.0003 (4) | 0.0016 (4) |
| | 0.0251 (3) | 0.0242 (4) | 0.0200 (4) | 0.0002 (2) | 0.0006 (2) | 0.0017 (3) |
| C(2) | 0.0201 (5) | 0.0193 (5) | 0.0169 (5) | 0.0021 (3) | −0.0007 (4) | 0.0035 (4) |
| | 0.0261 (2) | 0.0257 (3) | 0.0237 (2) | 0.0025 (2) | −0.0002 (2) | 0.0044 (2) |
| C(3) | 0.0194 (5) | 0.0159 (5) | 0.0194 (5) | 0.0044 (4) | 0.0041 (4) | 0.0025 (4) |
| | 0.0260 (2) | 0.0211 (3) | 0.0261 (2) | 0.0048 (2) | 0.0049 (2) | 0.0031 (2) |
| O(4) | 0.0183 (5) | 0.0136 (5) | 0.0162 (5) | 0.0015 (4) | 0.0032 (4) | −0.0003 (4) |
| | 0.0232 (3) | 0.0187 (3) | 0.0225 (3) | 0.0026 (3) | 0.0043 (2) | 0.0005 (3) |
| C(5) | 0.0226 (5) | 0.0129 (4) | 0.0173 (5) | 0.0010 (4) | 0.0041 (4) | −0.0000 (4) |
| | 0.0305 (3) | 0.0169 (3) | 0.0229 (2) | 0.0013 (2) | 0.0045 (2) | 0.0004 (2) |
| C(6) | 0.0199 (5) | 0.0157 (5) | 0.0175 (5) | −0.0043 (4) | 0.0047 (4) | 0.0005 (4) |
| | 0.0275 (3) | 0.0195 (3) | 0.0244 (2) | −0.0046 (2) | 0.0063 (2) | 0.0010 (2) |
| O(7) | 0.0159 (5) | 0.0167 (5) | 0.0177 (5) | −0.0021 (4) | 0.0038 (4) | 0.0019 (4) |
| | 0.0199 (3) | 0.0211 (3) | 0.0247 (2) | −0.0025 (3) | 0.0047 (2) | 0.0023 (4) |
| C(8) | 0.0157 (5) | 0.0186 (5) | 0.0250 (6) | −0.0029 (4) | 0.0030 (4) | −0.0000 (4) |
| | 0.0200 (2) | 0.0246 (3) | 0.0346 (3) | −0.0039 (2) | 0.0036 (2) | −0.0000 (2) |
| C(9) | 0.0174 (5) | 0.0196 (5) | 0.0198 (5) | 0.0006 (4) | −0.0010 (4) | −0.0004 (4) |
| | 0.0225 (2) | 0.0268 (3) | 0.0273 (3) | −0.0004 (2) | −0.0023 (2) | −0.0011 (2) |
| N(1) | 0.0221 (4) | 0.0182 (4) | 0.0157 (3) | −0.0029 (3) | 0.0050 (3) | −0.0002 (3) |
| | 0.0267 (3) | 0.0271 (4) | 0.0220 (4) | −0.0039 (3) | 0.0053 (3) | −0.0012 (4) |
| C(1) | 0.0249 (5) | 0.0190 (5) | 0.0200 (5) | 0.0050 (4) | 0.0103 (4) | 0.0039 (4) |
| | 0.0294 (4) | 0.0281 (5) | 0.0261 (5) | 0.0073 (3) | 0.0121 (3) | 0.0045 (4) |
| N(2) | 0.0566 (7) | 0.0341 (6) | 0.0401 (6) | 0.0165 (5) | 0.0332 (6) | 0.0188 (5) |
| | 0.0729 (9) | 0.0458 (7) | 0.0535 (8) | 0.0233 (7) | 0.0443 (7) | 0.0270 (6) |
| H(21) | 0.050 (2) | 0.037 (1) | 0.024 (1) | −0.002 (1) | 0.010 (1) | 0.001 (1) |
| H(22) | 0.031 (1) | 0.041 (2) | 0.048 (2) | 0.007 (1) | −0.010 (1) | 0.007 (1) |
| H(31) | 0.036 (1) | 0.040 (1) | 0.034 (1) | 0.002 (1) | 0.015 (1) | −0.004 (1) |
| H(32) | 0.041 (1) | 0.026 (1) | 0.046 (2) | 0.007 (1) | 0.001 (1) | 0.012 (1) |
| H(51) | 0.039 (1) | 0.038 (1) | 0.028 (1) | 0.004 (1) | 0.010 (1) | −0.008 (1) |
| H(52) | 0.049 (2) | 0.021 (1) | 0.040 (1) | −0.000 (1) | 0.000 (1) | 0.009 (1) |
| H(61) | 0.039 (1) | 0.025 (1) | 0.046 (2) | −0.012 (1) | −0.000 (1) | −0.001 (1) |
| H(62) | 0.039 (1) | 0.042 (2) | 0.028 (1) | 0.000 (1) | 0.014 (1) | 0.003 (1) |
| H(81) | 0.035 (1) | 0.044 (2) | 0.042 (2) | 0.007 (1) | 0.020 (1) | 0.006 (1) |
| H(82) | 0.032 (1) | 0.035 (1) | 0.059 (2) | −0.011 (1) | −0.008 (1) | −0.002 (1) |
| H(91) | 0.045 (2) | 0.036 (1) | 0.027 (1) | 0.003 (1) | 0.007 (1) | −0.003 (1) |
| H(92) | 0.026 (1) | 0.047 (2) | 0.050 (2) | 0.004 (1) | −0.012 (1) | 0.002 (1) |
| H(1) | 0.031 (1) | 0.047 (2) | 0.048 (2) | −0.011 (1) | 0.013 (1) | −0.003 (1) |
| H(2) | 0.047 (2) | 0.043 (2) | 0.023 (1) | 0.001 (1) | 0.002 (1) | 0.001 (1) |

[a] See footnote in Table III. [b] The temperature factor: $\exp\{-2\pi^2(h_i a^i)(h_j a^j)U^{ij}\}$, where $h_i$ and $a^i$ are reflection indices and reciprocal unit-cell edges, respectively.

**Table V.** Result of the Rigid-Body Motion Analysis Based on the Neutron Observation[a]

| | 18-crown-6 | | | cyanamide | | |
|---|---|---|---|---|---|---|
| tensor | | | | | | |
| | 148 (5) | 2 (4) | 16 (7) | 179 (47) | 11 (49) | 15 (22) |
| $T$ ($10^{-4}$ Å²) | | 138 (4) | 4 (5) | | 179 (26) | −24 (30) |
| | | | 115 (3) | | | 155 (26) |
| | 4 (1) | −1 (1) | 0 (1) | 94 (369) | −38 (397) | −70 (331) |
| $L$ ($10^{-4}$ rad²) | | 9 (1) | 0 (1) | | 151 (189) | −72 (110) |
| | | | 5 (1) | | | 270 (548) |
| $R$ | | 0.0972 | | | 0.0733 | |

[a] The maximal correction for bond length is 0.001 Å.

VII for both observations. To compare the molecular dimensions of the 18-membered ring in the title compound with those of the free polyether, the structural parameters of the uncomplexed form, taken from ref 15, are listed too. The present studies (N, X) gave a rather similar mean C–O distance (1.420 (2), 1.419 (1) Å) and slightly smaller mean C–O–C (112.3 (2)°, 112.3 (1)°) and O–C–C (108.8 (2)°, 108.7 (1)°) angles than the values obtained for the free ring (1.423 (1) Å, 112.8 (1)°, 109.3 (1)°, respectively). The mean C–C distances (1.509 (2), 1.506 (1) Å) appear to be short for a single aliphatic bond,[16] as found in previously published studies on cyclic ethers and their complexes [refs 15 and 17 and references therein]. From C(3) to C(8) an alternating sequence of shorter and longer bonds can be established. This arrangement can formally be interpreted as a result of a shortening in the C(3)–O(4) and C(8)–O(7) distances accompanied by a lengthening in the adjacent bonds. The polarization of the C–O bonds can be attributed to the dipole–dipole interaction between the complexed molecules. The six oxygen atoms are located alternately below (O(1), O(7), O(4)′) and above (O(1)′, O(7)′, O(4)) their common least-squares plane by about 0.23 Å (′ refers to equivalent atoms generated by the center of symmetry).

The crown can be characterized by the following sequence of partial conformations of the three successive –O–$CH_2$–$CH_2$–O– moieties: (–ap, sc, ap), (–ap, –sc, –ap), and (–ap, sc, –ap). The conformational changes in the polyether due to complexation are illustrated in Figure 3, where the complexed and the free ring are displayed fitted together (the mean square distance is 0.63 Å). The largest deviation appears around the trans corner of the free ring, where the corresponding ethyleneoxy unit of the complexed form possesses gauche conformation, characterized by a −68.9° torsion angle about the C(5)–C(6) bond.

(15) Maverick, E.; Seiler, P.; Schweizer, W. B.; Dunitz, J. D. *Acta Crystallogr.* **1980**, *B36*, 615.
(16) *Tables for Interatomic Distances and Configuration in Molecules and Ions*; Chemical Society Special Publications No. 11, Chemical Society: London, 1960.
(17) Goldberg, I. *Acta Crystallogr.* **1975**, *B31*, 754.

**Table VI.** Bond Distances (Å), Bond Angles (deg) and Torsion Angles (deg) in the 18-Crown-6 Molecule[a]

| atoms | | | | distance | angle | torsion angle |
|---|---|---|---|---|---|---|
| A | B | C | D | B–C | A–B–C | A–B–C–D |
| C(9)′ | O(1) | C(2) | C(3) | 1.420 (2) | 112.2 (2) | −176.3 (2) |
| | | | | 1.420 (1) | 112.2 (1) | −176.4 (1) |
| | | | | 1.423 (1) | 112.8 (1) | −154.9 (1) |
| O(1) | C(2) | C(3) | O(4) | 1.510 (2) | 108.7 (2) | 67.2 (2) |
| | | | | 1.508 (1) | 108.6 (1) | 67.0 (1) |
| | | | | 1.511 (1) | 110.2 (1) | 74.7 (1) |
| C(2) | C(3) | O(4) | C(5) | 1.410 (2) | 108.1 (2) | 178.1 (2) |
| | | | | 1.408 (1) | 108.3 (1) | 178.1 (1) |
| | | | | 1.425 (1) | 114.1 (1) | −80.3 (1) |
| C(3) | O(4) | C(5) | C(6) | 1.425 (2) | 112.6 (2) | −177.8 (2) |
| | | | | 1.422 (1) | 112.6 (1) | −177.9 (1) |
| | | | | 1.430 (1) | 113.0 (1) | −169.2 (1) |
| O(4) | C(5) | C(6) | O(7) | 1.505 (1) | 108.4 (2) | −68.9 (2) |
| | | | | 1.503 (1) | 108.6 (1) | −68.6 (1) |
| | | | | 1.512 (1) | 108.3 (1) | −173.7 (1) |
| C(5) | C(6) | O(7) | C(8) | 1.426 (2) | 109.3 (2) | −175.8 (2) |
| | | | | 1.426 (1) | 109.2 (1) | −176.2 (1) |
| | | | | 1.422 (1) | 105.5 (1) | −172.4 (1) |
| C(6) | O(7) | C(8) | C(9) | 1.414 (2) | 112.1 (2) | −179.0 (2) |
| | | | | 1.414 (1) | 112.0 (1) | −179.2 (1) |
| | | | | 1.418 (1) | 112.7 (1) | −175.2 (2) |
| O(7) | C(8) | C(9) | O(1)′ | 1.513 (2) | 109.3 (2) | 69.6 (2) |
| | | | | 1.506 (1) | 109.1 (1) | 69.6 (1) |
| | | | | 1.506 (1) | 108.3 (1) | 65.1 (1) |
| C(8) | C(9) | O(1)′ | C(2)′ | 1.422 (1) | 108.7 (1) | −179.0 (1) |
| | | | | 1.426 (1) | 108.6 (1) | −179.3 (1) |
| | | | | 1.421 (1) | 109.6 (1) | −165.6 (1) |

[a] Upper line, neutron refinement; middle line, X-ray multipole refinement; lower line; from ref 16.

**Table VII.** Bond Distances (Å), Bond Angles (deg) and Torsion Angles (deg) in the Cyanamide Molecule[a]

| atoms | | | | distance | angle | torsion angle |
|---|---|---|---|---|---|---|
| A | B | C | D | B–C | A–B–C | A–B–C–D |
| H(1) | N(1) | C(1) | N(2) | 1.321 (1) | 119.2 (4) | 136.0 (4) |
| | | | | 1.322 (2) | 120.5 (4) | 138.2 (5) |
| | | | | 1.315 (1) | 123.6 (7) | |
| | | | | 1.346 | 115.6 | |
| H(2) | N(1) | C(1) | N(2) | | 116.4 (3) | −81.6 (4) |
| | | | | | 116.3 (3) | −79.3 (4) |
| | | | | | 115.8 (9) | |
| | | | | | 115.6 | |
| N(1) | C(1) | N(2) | | 1.156 (2) | 175.0 (2) | |
| | | | | 1.159 (2) | 175.0 (2) | |
| | | | | 1.152 (1) | 178.1 (1) | |
| | | | | 1.16 | 180.0 | |
| H(1) | N(1) | H(2) | | 1.008 (3) | 113.7 (5) | |
| | | | | 1.006 (3) | 112.8 (5) | |
| | | | | 0.90 (1) | 117 (1) | |
| | | | | 1.001 | 113.5 | |
| H(2) | N(1) | H(1) | | 1.009 (3) | | |
| | | | | 1.023 (3) | | |
| | | | | 0.88 (1) | | |
| | | | | 1.001 | | |

[a] Entries from upper to lower line refer to neutron, X-ray multipole refinement, X-ray study,[19] and gas-phase microwave measurement.[20]

The observed geometrical parameters of the cyanamide molecule (Table VII) can be compared to previous room-temperature X-ray data[18] and those predicted from a gas-phase microwave measurement.[19] Due to intermolecular forces the expected $C_s$ symmetry of the cyanamide molecule is destroyed. This structural deformation can be described as a bending of the N(1)–C(1)–N(2) angle, accompanied by an internal rotation of the $NH_2$ group around the N(1)–C(1) axis. The obtained C(1)–N(2) bond length of 1.156 (2) Å is significantly longer than that of 1.136 (10) Å given in ref 20 as an overall C(sp1)≡N distance, averaged over 140 entries of nitrile derivatives found in the Cambridge Structural Database. It is though in good agreement with the value of 1.160 (1) Å obtained by neutron diffraction for tetracyanoethylene.[21] In many nitrile derivatives the analogous —C—C≡N fragment was found to be nonlinear.[22,23]

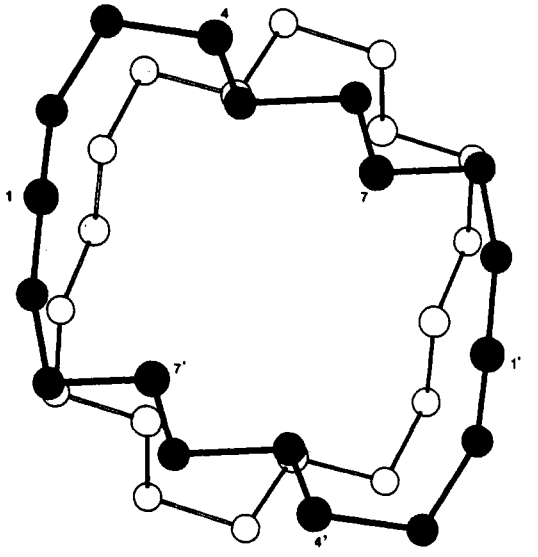


**Figure 3.** PLUTO drawing of the free and complexed ring fitted together by minimizing the distances of the equivalent oxygen atoms: shaded circles, free ring; open circles, complexed ring.

(18) Denner, L.; Luger, P.; Buschmann, J. *Acta Crystallogr.* **1988**, *C44*, 1979.
(19) Tyler, J. K.; Sheridan, J. *J. Mol. Spectrosc.* **1972**, *43*, 24.
(20) Allen, F. H.; Kennard, O.; Watson, D. G.; Brammer, L.; Orpen, A. G.; Taylor, R. *J. Chem. Soc., Perkin Trans II* **1987**, 1.
(21) Becker, P.; Coppens, P.; Ross, F. K. *J. Am. Chem. Soc.* **1973**, *95*, 7604.
(22) Begley, J. M.; Harper, A.; Hubberstey, P. *J. Chem. Res., Synop.* **1979**, 398.

**Table VIII.** Hydrogen Bonds and Nonbonded Interactions ($X\cdots Y < W_X + W_Y$, $H\cdots Y < W_H + W_Y - 0.3$, $X\text{-}Y\cdots H > 100°$)[a]

| interaction X-Y···Z | distance (Å) Y···Z | distance (Å) X···Z | angle (deg) X-Y···Z | equiv positions & translation | |
|---|---|---|---|---|---|
| N(1)-H(1)···O(7) | 2.042 (4) | 3.005 (4) | 158.8 (2) | (1) | [0,0,0] |
| N(1)-H(2)···O(1) | 1.978 (3) | 2.970 (3) | 167.6 (2) | (1) | [0,0,0] |
| N(1)-H(2)···C(3) | 2.848 (3) | 3.473 (3) | 120.8 (2) | (1) | [0,0,0] |
| C(6)-H(61)···N(2) | 2.621 (3) | 3.450 (3) | 131.3 (2) | (2) | [0,0,0] |
| N(1)-H(1)···C(5) | 3.044 (4) | 3.480 (4) | 107.3 (2) | (1) | [0,0,0] |
| N(1)-H(1)···C(6) | 3.043 (4) | 3.828 (4) | 135.4 (2) | (1) | [0,0,0] |
| N(1)-H(2)···C(2) | 2.902 (3) | 3.815 (3) | 151.0 (2) | (1) | [0,0,0] |
| C(5)-H(52)···N(1) | 2.684 (3) | 3.752 (3) | 162.9 (2) | (4) | [-1,0,-1] |
| C(6)-H(61)···N(2) | 2.621 (3) | 3.450 (3) | 131.3 (2) | (2) | [0,0,0] |
| C(9)-H(91)···N(2) | 2.466 (3) | 3.547 (3) | 166.2 (2) | (3) | [0,0,0] |
| C(9)-H(92)···N(2) | 2.539 (3) | 3.599 (3) | 161.5 (2) | (1) | [1,-1,0] |
| C(5)-H(51)···C(3) | 2.855 (3) | 3.912 (3) | 162.1 (2) | (4) | [0,0,0] |
| C(5)-H(51)···C(5) | 2.992 (3) | 2.945 (3) | 149.3 (2) | (4) | [0,0,0] |
| C(6)-H(62)···C(1) | 3.042 (3) | 3.671 (3) | 116.8 (2) | (3) | [0,0,0] |
| C(9)-H(92)···C(1) | 2.760 (3) | 3.765 (3) | 151.6 (2) | (1) | [1,-1,0] |
| N(2)···C(5) | 3.351 (2) | | | (2) | [-1,-1,0] |
| N(2)···C(6) | 3.450 (2) | | | (2) | [-1,-1,0] |
| C(1)···O(4) | 3.265 (2) | | | (3) | [0,-1,0] |

[a] Van der Waals radii are those given by Allinger[28] ($W_H$ = 1.5 Å, $W_C$ = 1.75 Å, $W_O$ = 1.65 Å, $W_N$ = 1.7 Å). Equivalent positions for $P2_1/c$ are referred: (1) $x, y, z$; (2) $-x, {}^1/_2 + y, {}^1/_2 - z$; (3) $-x, -y, -z$; (4) $x, {}^1/_2 - y, {}^1/_2 + z$.

**Table IX.** Significant Multipole Populations ($P_{lm} \geq \sigma(P_{lm})$) and Screening Constants for the 18-Crown-6 Molecule

| | | O(1) | O(4) | O(7) | C(2-9) | H(C) |
|---|---|---|---|---|---|---|
| | | 0.98 | 0.98 | 0.98 | 0.96 | 1.0 |
| $P_v$ | | 6.10 | 6.06 | 6.03 | 4.36 | 0.79 |
| $l$ | $m$ | | | | | |
| 1 | 1 | -0.06 | -0.04 | -0.07 | -0.07 | 0.13 |
| 1 | -1 | -0.11 | -0.08 | -0.08 | -0.06 | |
| 2 | 0 | 0.13 | 0.12 | 0.09 | 0.07 | |
| 2 | 2 | -0.05 | 0.04 | -0.05 | -0.05 | |
| 2 | -2 | 0.11 | 0.05 | 0.06 | 0.02 | |
| 3 | 1 | | -0.03 | | -0.18 | |
| 3 | -1 | -0.02 | -0.02 | -0.02 | -0.26 | |
| 3 | 3 | 0.11 | 0.07 | 0.09 | 0.24 | |
| 3 | -3 | 0.01 | 0.01 | | 0.08 | |
| 4 | 0 | 0.01 | 0.02 | 0.02 | 0.02 | |
| 4 | 2 | | -0.02 | -0.02 | -0.07 | |
| 4 | -2 | 0.01 | | 0.01 | 0.15 | |
| 4 | 4 | | 0.02 | | 0.07 | |
| 4 | -4 | | -0.01 | | 0.01 | |

**Table X.** Significant Multipole Populations and Screening Constants for the Cyanamide Molecule

| | | C(1) | N(1) | N(2) | H(1,2) |
|---|---|---|---|---|---|
| | | 1.01 | 0.97 | 0.97 | 1.0 |
| $P_v$ | | 3.41 | 5.53 | 6.00 | 0.63 |
| $P_a$[a] | | 3.47 | 5.45 | 5.90 | 0.59 |
| $l$ | $m$ | | | | |
| 1 | 1 | -0.32 | -0.14 | 0.45 | 0.06 |
| 1 | -1 | 0.05 | | -0.11 | |
| 1 | 0 | -0.04 | | 0.05 | |
| 2 | 0 | -0.05 | 0.12 | -0.36 | |
| 2 | 1 | -0.11 | -0.11 | -0.11 | |
| 2 | -1 | 0.04 | 0.11 | | |
| 2 | 2 | | -0.11 | 0.38 | |
| 2 | -2 | 0.12 | 0.12 | -0.10 | |
| 3 | 0 | | 0.12 | 0.06 | |
| 3 | 1 | 0.18 | -0.14 | -0.15 | |
| 3 | -1 | -0.02 | -0.02 | 0.03 | |
| 3 | 2 | | 0.04 | -0.07 | |
| 3 | -2 | -0.02 | -0.08 | -0.03 | |
| 3 | 3 | -0.24 | 0.07 | 0.13 | |
| 3 | -3 | -0.05 | -0.03 | 0.05 | |
| 4 | 0 | -0.05 | 0.01 | | |
| 4 | 1 | 0.05 | -0.05 | | |
| 4 | -1 | 0.02 | | 0.04 | |
| 4 | 2 | 0.05 | | -0.15 | |
| 4 | -2 | -0.03 | 0.02 | | |
| 4 | 3 | -0.06 | -0.05 | | |
| 4 | -3 | | 0.03 | | |
| 4 | 4 | -0.07 | | 0.10 | |
| 4 | -4 | 0.11 | -0.01 | -0.02 | |

[a] Pa: from ab initio (6-31G*) calculation.

**Molecular Packing.** The two cyanamide molecules are attached above and below the crown via hydrogen bonds. The crown's mean plane forms -70.7° and 63.0° dihedral angles with the $NH_2$ and N(1)-C(1)-N(2) plane, respectively, and is nearly parallel to and about ±1.2 Å away from the H(1)-H(2) and H(1)′-H(2)′ lines.

The geometrical values for various intermolecular close contacts based on the neutron observation are listed in Table VIII. The leading forces of complexation are the N-H···O hydrogen bonds from the cyanamide hydrogen to the ether oxygen atoms (O(1), O(7)); O···H distances of about 2 Å indicate interactions of intermediate strength. Accepting the criteria proposed by W. C. Hamilton and J. A. Ibers,[24] two additional very weak hydrogen bonds can be assigned to the structure. The cyanamide molecules, having donor as well as acceptor nitrogen atoms, connect the crowns via an O···H-N(1)-C(1)-N(2)···H bonding pattern forming an infinite chain.

In the observed geometrical arrangement more H-centered contacts with weak "hydrogen bond-like" interactions can be established. In addition, significant interactions of N···C type with a typical distance of 3.4 Å can be found. They are similar in distance and orientation to contacts observed in crystal structures of several nitrile compounds.[25]

**Deformation Densities.** Electron migrations due to chemical bonds are usually shown by deformation electron density calculated as the difference between the total molecular and the superposed isolated atomic charge distributions. To obtain experimental deformation density the most commonly used procedure is to calculate the following Fourier summation (X-X synthesis)

$$\rho(r) = (2/V)\sum_H (F_{obs}(H) - F_{sph}(H)) \exp(-2\pi i H r)$$

(23) Begley, J. M.; Harper, A.; Hubberstey, P. *J. Chem. Res., Miniprint* **1979**, 4620.

(24) Hamilton, W. C.; Ibers, J. A. *Hydrogen Bonding in Solids*; W. Benjamin, Inc.: New York, 1968.

(25) Britton, D.; Gleason, W. B. *Cryst. Struct. Commun.* **1982**, *11*, 1155.

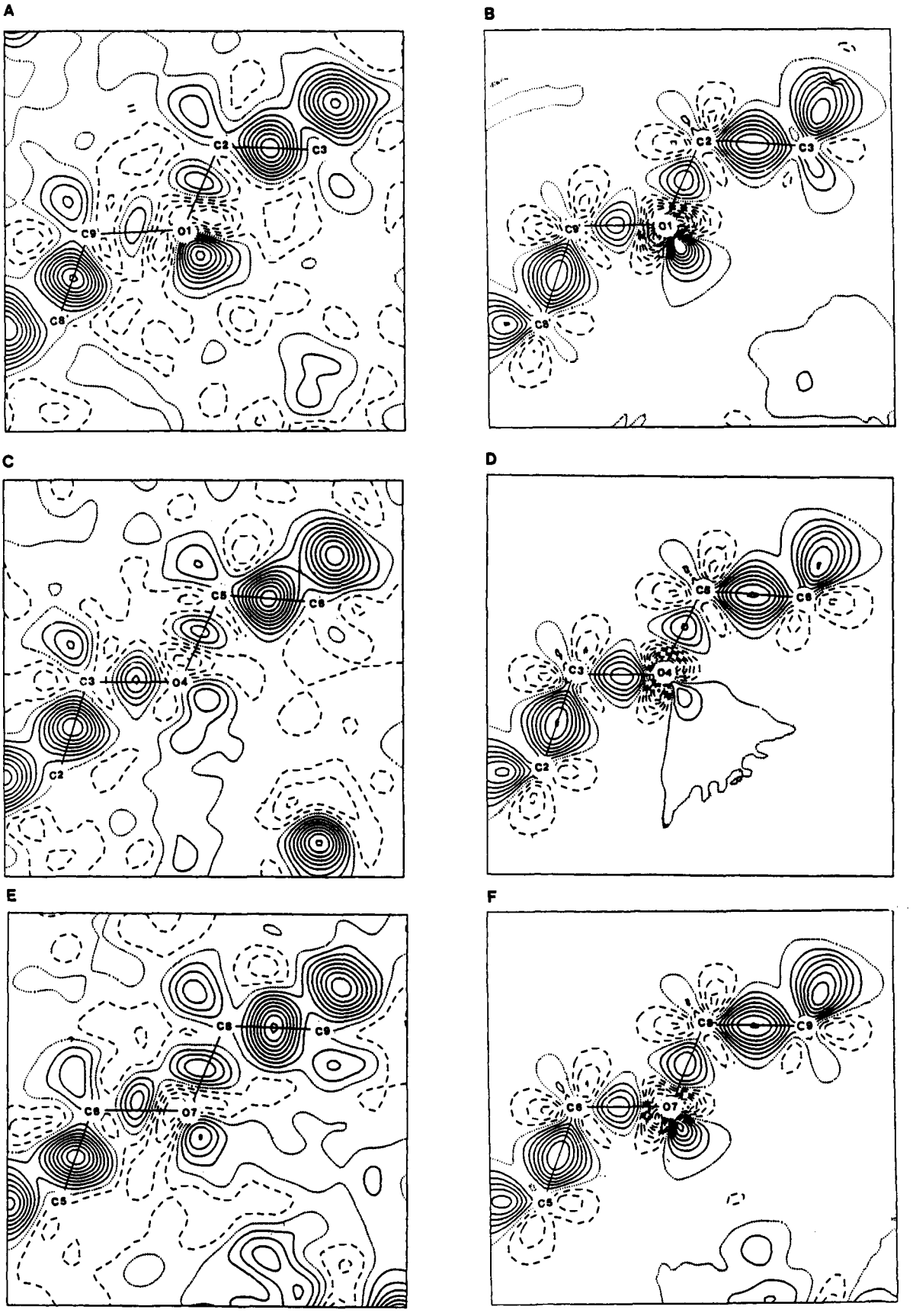


**Figure 4.** Plots of dynamic (left) and static (right) deformation densities calculated in the three C–O–C planes: (A,B) C(9)–O(1)–C(2), (C,D) C(3)–O(4)–C(5), and (E,F) C(6)–O(7)–C(8).

where $F_{obs}$ and $F_{sph}$ are the observed and calculated structure factors, respectively. In the present study $F_{sph}$ is generated from spherically averaged atoms defined by the positional and thermal parameters obtained after multipole refinement, and the phase is given by the sign of $F_{mul}$ (aspherical structure factor based on multipole expansion). The dynamic deformation density (DDD), obtained in such a way, represents a distribution of charge averaged over the nuclear motion. The aspherical refinement leads

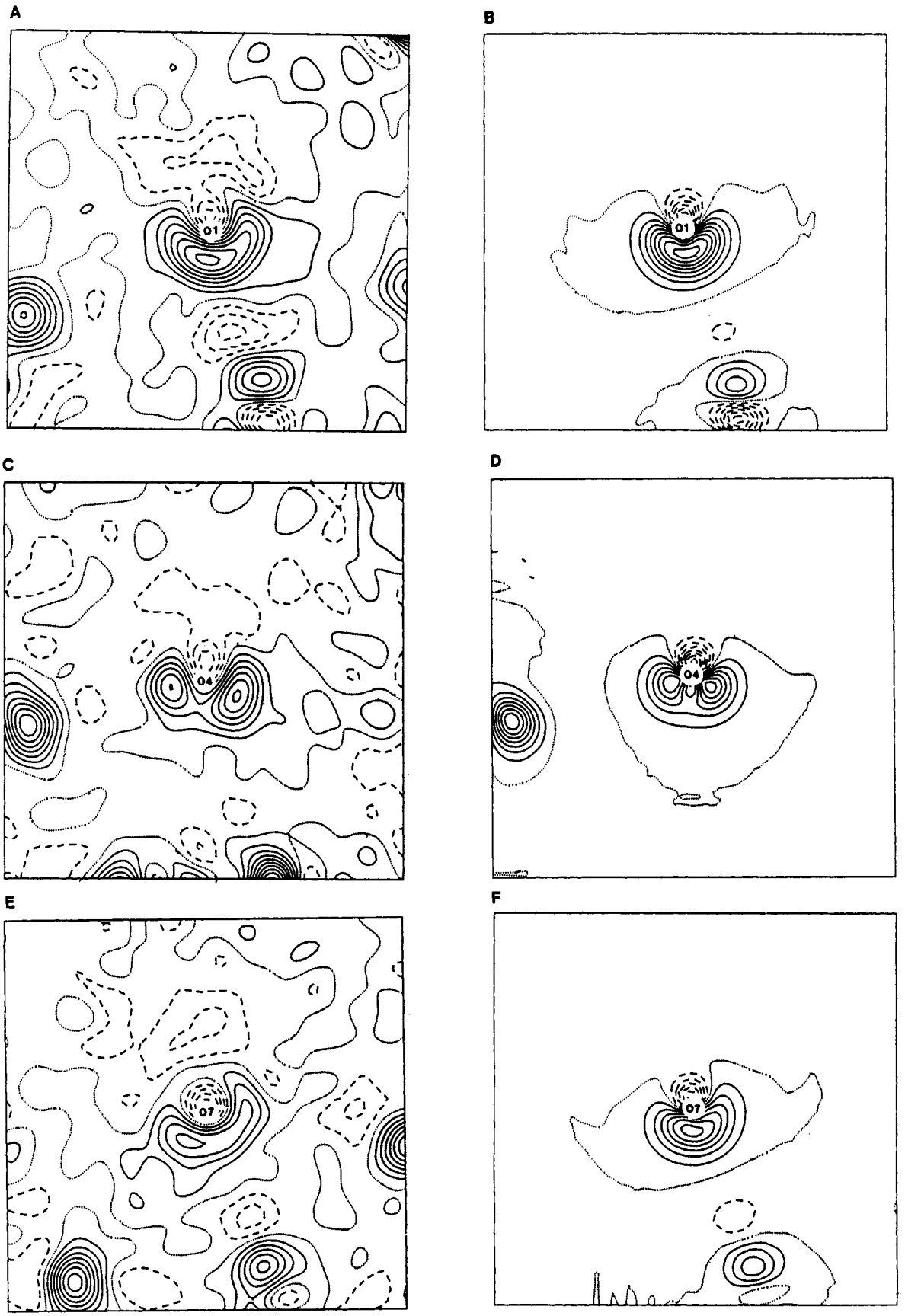


**Figure 5.** Plots of dynamic (left) and static (right) deformation densities in the planes bisecting the three C–O–C angles: (A,B) O(1), (C,D) O(4), and (E,F) O(7).

to a model density expressed in terms of spherical harmonics. From this function the static deformation density (SDD) can be calculated which represents a difference distribution extrapolated to zero thermal motion. To decrease the experimental noise from the lower statistical accuracy of the high-angle reflections, only the low-order data ($\sin\theta/\lambda \leq 0.8$ Å$^{-1}$) with $F_{obs} \geq 3\sigma(F_{obs})$ were included in the Fourier summation. In all of the presented DDD sections the standard deviation is estimated to be smaller than

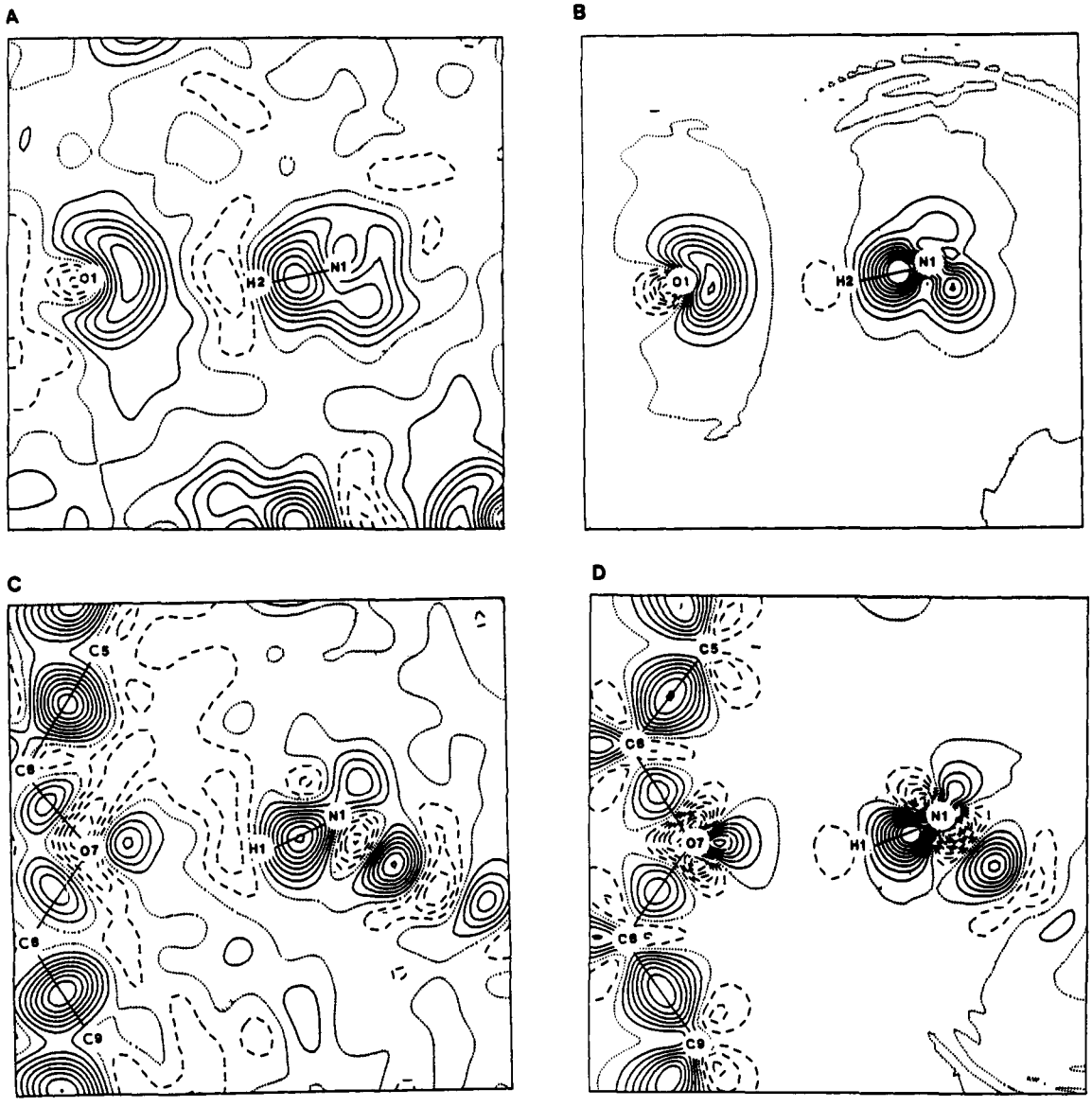


Figure 6. Plots of dynamic (left) and static (right) deformation densities in the N–H···O planes: (A,B) N(1)–H(2)···O(1) and (C,D) N(1)–H(1)···O(7).

0.03e/Å$^3$ for any general position. Contour intervals are 0.05 and 0.1e/Å$^3$ for DDD and SDD, respectively.

## Discussion

The final, significant multipole populations for the crown and the cyanamide molecule are given in Tables IX and X. Since all oxygen atoms are found to be nearly neutral, the −0.36 e net charge on each carbon atom is mainly at the expense of the charge at the hydrogen atoms. Comparing the multipole populations of the oxygen atoms, the main difference appears in $P_{2-2}$ which is significantly larger for O(1) than for the other two oxygen atoms. In the applied site coordinate system this term corresponds to the population of the $P_xP_y$ orbital product which has positive lobes in the C–O–C plane in the bisecting direction. This density accumulation yields overlapping lone-pair peaks that can be attributed to the effect of polarization caused by the hydrogen bond.

As expected, the density populations of the N–C–N fragment show evidence for $\pi$ orbitals. Ab initio calculation with the (6–31G*) basis set was performed on the cyanamide molecule. The nuclear positions were those obtained experimentally, i.e., part of the effect of the complexation on the cyanamide was implicitly included. The comparison of the net valence charges given by multipole refinement to those theoretically calculated reveals good agreement (Table X).

Plots of DDD and SDD calculated in the three different C–O–C planes are displayed in Figure 4 (parts A, C, and E and parts B, D, and F, respectively). Well-defined bond peaks appear which are higher in the C–C than in the C–O bonds. The density deformation around O(4) (Figure 4C,D) supports the geometrical asymmetry of the C(3)–O(4)–C(5) unit. An area with a pronounced charge depletion appears in the direction of the longer bond. In addition, the $\sigma$ lone-pair peak is weaker than for the other two oxygen atoms. A certain deviation from the bisecting mirror symmetry is also observable for O(7) (Figure 4E,F), but it is not as pronounced as for O(4). Here the C–O bond peaks appear to be balanced by the enrichment of the lone-pair region of O(7) in comparison to that of O(4), which is probably due to the nearby proton. To further examine the reason for the bond shortenings, the deformations were calculated in the planes perpendicular to each bond. No deviation from the expected circular symmetry was observed. This indicates that the change in the bond length is the result of an inductive effect and not due to a $\pi$ character of the bond.

DDD and SDD, calculated in the plane bisecting the C(3)–O(4)–C(5) angle (Figure 5C,D), show two distinct density maxima which can be assigned to the lone-pair electrons. In contrast to this situation in the corresponding sections for O(1) and O(7) (Figure 5 (parts A,B and E,F, respectively)) which take part in hydrogen bonds, only one contiguous lone-pair lobe appears, indicating charge concentration toward the proton.

Deformations, calculated in the planes formed by the N–H···O bridges (Figure 6), show no evidence of density accumulation

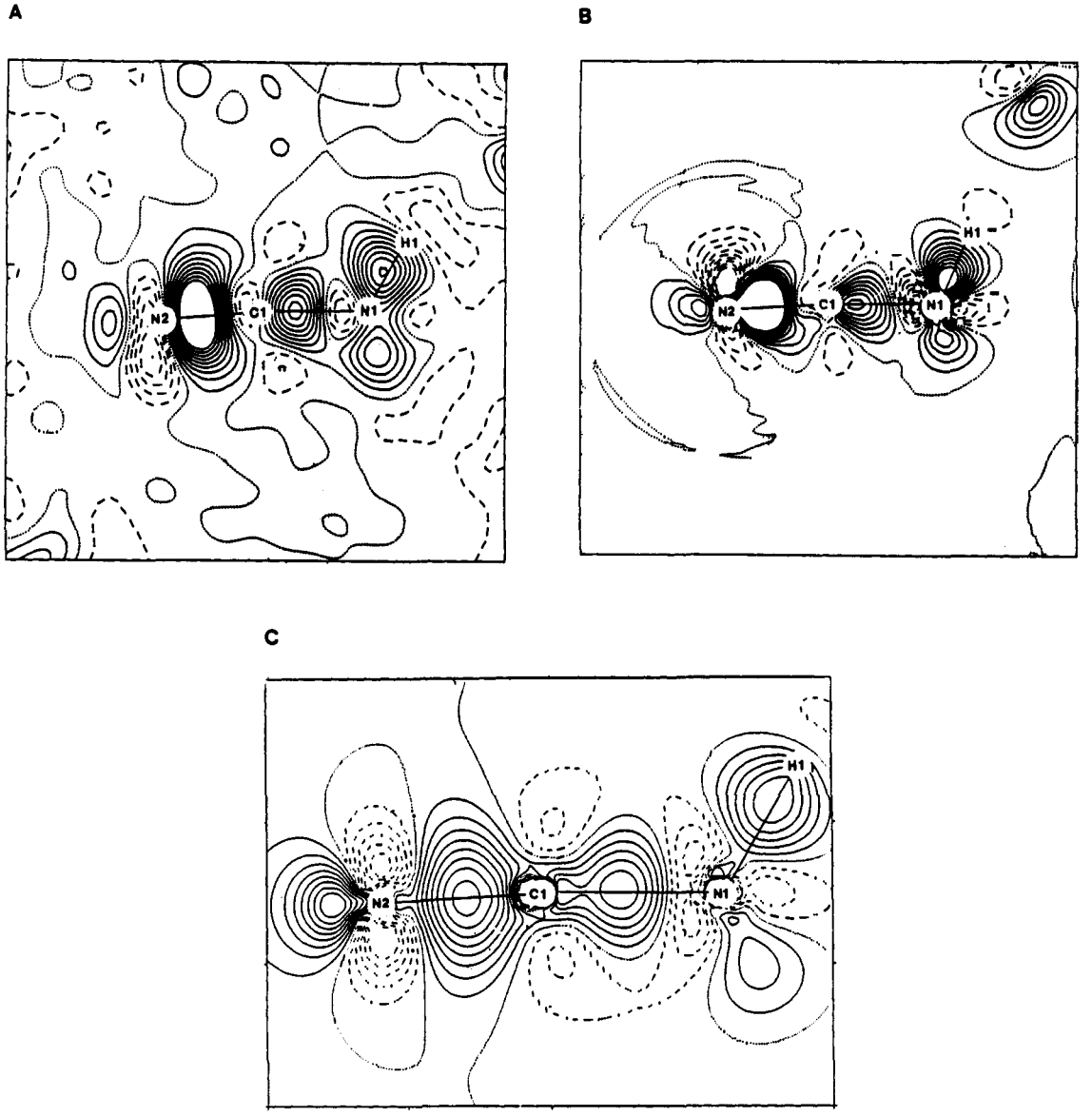


**Figure 7.** Plots of deformation densities of the cyanamide molecule in the C(1)–N(1)–H(1) plane: (A) dynamic, (B) static, and (C) theoretical (6-31G*).

midway between the proton and the acceptor. This supports the hypothesis that the main contribution to the interaction is purely electrostatic, as it is observed in many cases for weak hydrogen bonds. In addition, electron-deficient areas around the central hydrogen atoms can be recognized, which are usually interpreted as the result of increased polarization of the X–H bond in the field of lone-pair electrons of Y, forming an X–H···Y hydrogen bond.

Figures 7A–C display the DDD, SDD, and theoretical maps calculated in the C(1)–N(1)–H(1) plane. They are topologically similar, and the difference between the observed and theoretical maps can partly be attributed to crystal field effects on the charge density.

In order to see how the polyether bond length alternation pattern and the observed local asymmetry in the deformation density are related in terms of dipole–dipole forces, the total electronic dipole moment of the cyanamide ($d_g$) and the crown ($d_h$, for the asymmetric unit) were calculated from the multipole populations.[26] In addition, the dipole moments of all $CH_2$–O($n$)–$CH_2$ units ($d_n$, $n$ = 1, 4, 7) were also evaluated to decompose the total moment into local contributions. The dipole–dipole forces can be characterized by six parameters: the absolute values of the dipole moment vectors, the separation of their origins taken at the center of mass of the interacting fragments, and three angles ($\theta_A$, $\theta_B$, $\alpha$) to describe their mutual orientation (Table XI). The $d_h$–$d_g$ orientation is that expected from the molecular packing. The dipole moments of the subsequent $CH_2$–O($n$)–$CH_2$ groups of approximately equal magnitude are in the corresponding C–O(n)–C plane, nearly in bisecting positions. Two basically different geometrical arrangements of $d_g$ and the local components of $d_h$ can be established. The plane defined by the $d_1$ and $d_g$ vectors almost coincides with the C(9)′–O(1)–C(2) bisecting plane, leading to a nearly symmetrical orientation of $d_g$ with respect to the C–O bonds. In contrast, for the other two $CH_2$–O–$CH_2$ groups, the dipole–dipole interaction takes place in such a way that the $d_g$ vector has a larger component along one of the bonds, which becomes more polarized due to an inductive effect than the other. The latter two arrangements seem to resemble the observed asymmetry in the geometry as well as in the deformation density

**Table XI.** Dipole–Dipole Interactions[a]

| A | B | $d_A$ | $d_B$ | $R_{AB}$ | $\theta_A$ | $\theta_B$ | $\alpha$ |
|---|---|---|---|---|---|---|---|
| $d_g$ | $d_h$ | 5.54 | 7.25 | 3.54 | 15.5 | 137.4 | −178.4 |
| $d_g$ | $d_1$ | | 4.64 | 4.14 | 42.9 | 172.4 | 101.8 |
| $d_g$ | $d_4$ | | 4.44 | 4.31 | 23.3 | 110.5 | −174.9 |
| $d_g$ | $d_7$ | | 4.52 | 4.46 | 38.3 | 171.9 | −52.2 |

[a] $d_A$ and $d_B$ are the dipole moments ($D$) of fragments A and B at the distance of $R_{AB}$ (Å); $\theta_A$ and $\theta_B$ are the $Rd_A$ and $Rd_B$ angles (deg), respectively; $\alpha$ is the torsion angle (deg).

(26) Coppens, P.; Hansen, N. K. *Isr. J. Chem.* **1977**, *16*, 163.
(27) Allinger, N. L. Calculations of Molecular Structure and Energy by Force-Field Methods. *Adv. Phys. Org. Chem.* **1976**, *13*, 1–82.

of the C(3)-O(4)-C(5) and C(6)-O(7)-C(8) fragments.

**Results and Conclusions**

The presented low-temperature X-ray and neutron study on the complex of 18-crown-6 with two cyanamides shows that the bonding between the molecules consists, on the one hand, of hydrogen bridges and, on the other hand, of dipole–dipole interactions. As a result of these forces the "chemical symmetries", characteristic for the isolated molecules, are not preserved in the complex. Asymmetries are present in the molecular geometry as well as in the local features of the deformation density.

The N-H···O hydrogen bonds lead to extra charge concentration in the lone-pair region of the participating oxygen atoms in the direction of the proton. This excess density can formally be described as an enrichment in the distribution of the $\sigma$ nonbonded orbital. As a result, only one maximum is found in the electron deformation density, calculated in the bisecting plane of the C–O–C angle. In contrast, the oxygen atom, which is not involved in a hydrogen bond, exhibits distinct lone-pair peaks. As there is no further charge accumulation between the donor and the acceptor, the hydrogen bond can be characterized as mainly an electrostatic interaction.

The significantly varying bond lengths indicate that some of the C–O bonds in the crown are more polarized than others. The stronger bonds exhibit a higher charge density midway between the atoms. The valence deformation of the oxygen atom in a nonsymmetric C–O–C fragment has a more depleted area in the longer than in the shorter bond. The analysis of the dipole–dipole interactions in terms of dipole moments, calculated from the multipole populations, revealed that these asymmetries in the crown are induced by the electric field of the cyanamide molecule.

In order to analyze the details of the host–guest interactions in crown ether complexes with ionic guests also, further experimental charge density studies are being undertaken.

**Acknowledgment.** We gratefully acknowledge the substantial support of this work by a grant from the Bundesminister für Forschung und Technologie under contract No. 03-Lu1FUB-0-D1-58 and financial assistance by the Fonds der Chemischen Industrie. We thank the ILL, Grenoble, for providing the neutron beam facilities. Experimental help was given by David Gregson.

**Registry No.** 18-Crown-6·2 cyanamide, 87157-16-2.

# Effects of Structural Changes on Acidities and Homolytic Bond Dissociation Energies of the H–N Bonds in Amidines, Carboxamides, and Thiocarboxamides

**Frederick G. Bordwell* and Guo-Zhen Ji**

*Contribution from the Department of Chemistry, Northwestern University, 2145 Sheridan Road, Evanston, Illinois 60208-3113.* *Received April 3, 1991*

**Abstract:** The equilibrium acidities in DMSO have been measured for acetamidine, benzamidine, *N,N'*-diphenylbenzamidine, *N,N*-diethylbenzamidine, diphenylmethanimine, guanidine, *N,N'*-diphenylguanidine, *N,N'*-diphenylurea, and *N,N'*-diphenylthiourea. Combination of the resulting $pK_{HA}$ values for these weak acids with the oxidation potentials of their conjugate bases gave estimates of their homolytic bond dissociation energies (BDEs). These acidities and BDEs are compared with those of the corresponding carboxamides and thiocarboxamides. The change in hybridization of nitrogen between $NH_3$ and $Ph_2C{=}NH$ causes the acidities and BDEs to increase by about 14 and 9 kcal/mol, respectively. These changes are similar to the increases in gas-phase acidities and BDEs observed for the change in hybridization between $CH_3CH_3$ and $CH_2{=}CH_2$ (12 and 12 kcal/mol, respectively). The BDE of the H–N bond in $HN_3$ is about 25 kcal/mol lower than that in $Ph_2C{=}NH$, despite the apparent similarities in hybridization. The acidities of the H–N bonds in acetamide, benzamide, and urea are 2.2, 4.6, and 2.2 kcal/mol higher than those of the H–N bonds in acetamidine, benzamidine, and guanidine, respectively, and their BDEs are 6, 5, and 7 kcal/mol higher. The acidities of the H–N bonds in thioacetamide, thiobenzamide, and thiourea are 9.6, 8.8, and 8.1 kcal/mol higher than those of the H–N bonds in acetamide, benzamide, and urea, respectively, and their BDEs are 17, 16, and 18 kcal/mol lower. The 6 kcal/mol lower BDEs for the H–N bonds in acetamidine and benzamidine than in ammonia point to the presence of resonance energy in $HN^{\bullet}C(R){=}NH$ radicals in contrast to its near absence in $HN^{\bullet}C(R){=}O$ radicals.

In the gas phase, the acidity of the H–C bond in the series $H_3CCH_3$ (413) < $H_2C{=}CH_2$ (401) < $HC{\equiv}CH$ (370) is known to increase as the s-character of carbon increases along the series, as shown.[1] (The numbers in parentheses are gas-phase acidities, kcal/mol; henceforth, kcal/mol will be abbreviated as kcal.) At the same time, the homolytic bond dissociation energies (BDEs) of the H–C bonds increase from 98 to 110 to 132 kcal.[2,3] One would expect the heterolytic and homolytic bond dissociation energies of H–N bonds to show the same reverse trends with changes in hybridization of nitrogen, but there appears to be no literature addressing this point.[4] The two nitrogen atoms in acetamidine (**1**) are in different states of hybridization, and our

(1) Bartmess, J. E. Table of homolytic X–H bond strengths pertinent to the 1990 gas-phase acidity scale. A copy of this table may be obtained from Prof. J. E. Bartmess, Department of Chemistry, University of Tennessee, Knoxville, TN 37996.

(2) Ervin, K. M.; Gronert, S.; Barlow, S. E.; Giles, M. K.; Harrison, A. G.; Bierbaum, V. M.; DePuy, C. H.; Lineberger, W. C.; Ellison, G. B. *J. Am. Chem. Soc.* **1990**, *112*, 5750–5759.

(3) Janousek, B. K.; Brauman, J. I.; Simons, J. *J. Chem. Phys.* **1979**, *71*, 2057–2061.

(4) There is a paucity of data available on the acidities and BDEs of H–N bonds. McMillen and Golden give BDE values for H–N bonds in only 7 compounds,[5] and Bartmess includes only 6 more in a list of 103 H–A bonds.[1] To the best of our knowledge, no measurements of the acidities or BDEs of the H–N bonds in amidines, guanidine, or imines have appeared in the literature.

(5) McMillen, D. F.; Golden, D. M. *Annu. Rev. Phys. Chem.* **1982**, *33*, 493–532.

0002-7863/91/1513-8398$02.50/0 © 1991 American Chemical Society